Journal of Materials Chemistry C

Supplementary Information

Enhanced Dielectric Performance of Amorphous Calcium Copper Titanate/Polyimide Hybrid Film

Qingguo Chi,[*a,b,c] Jia Sun,[b] Changhai Zhang,[b] Gang Liu,[b] Jiaqi Lin,[b] Yuning Wang,[a] Xuan Wang,[a] and Qingquan Lei[a]

[a] *Key Laboratory of Engineering Dielectrics and Its Application, Ministry of Education, Harbin University of Science and Technology, Harbin 150080, P. R. China*

[b] *School of Applied Science, Harbin University of Science and Technology, Harbin 150080, P. R. China*

[c] *State Key Laboratory of Electrical Insulation and Power Equipment, Xi'an Jiaotong University, Xi'an 710049, P.R. China*

Synthesis of *a*-CCTO and CCTO ceramics

In this study, *a*-CCTO ceramics were prepared using sol-gel technology and $Ca(NO_3)_2{\cdot}4H_2O$ (≥99%, 7.0845 g), $Cu(NO_3)_2{\cdot}3H_2O$ (≥98%, 21.7440 g), $[CH_3(CH_2)_3O]_4Ti$ (≥98%, 40.9 ml) and ethylene glycol monomethyl ether ($C_3H_8O_2$, ≥99%, 160 ml) as solvent. CCTO sol (0.15 mol L^{-1}) preparation was the first step. Pre-calculated amounts of $Ca(NO_3)_2{\cdot}4H_2O$ and $Cu(NO_3)_2{\cdot}3H_2O$ were mixed and dissolved in the solvent with heating (60 °C) and stirring for 30 min to yield a baby blue solution, upon which the solution was cooled to room temperature. Subsequently, $[CH_3(CH_2)_3O]_4Ti$ was added to the stirred solution and the reaction allowed to continue for 1 h at room temperature to obtain a transparent blue sol with the chemical composition $CaCu_3Ti_4O_{12}$. The resulting sol was stored for 24 h and was then kindled to obtain black gel powders. The prepared powders were milled using an agate mortar and a small amount of powder was cold pressed into disks of 10 mm in diameter and

* Corresponding author: Ph.D Qingguo Chi, E-mail: qgchi@hotmail.com Tel/Fax: +86-451-86391681

0.8 mm in thickness under a pressure of 14 MPa for 1.5 min. Finally, the obtained disks and gel powders were sintered at 300 °C in an air atmosphere and heated at 5 °C min^{-1} and then furnace-cooled to room temperature. The *a*-CCTO disks were used to evaluate the dielectric properties. The prepared powders were ball-milled (600 r min^{-1}) for 4 h in a planetary mill using an agate container and these were used as *a*-CCTO fillers. Crystalline $CaCu_3Ti_4O_{12}$ disks and powders were prepared using the same method apart from sintering at 1050 °C.

Characterization of *a*-CCTO and CCTO ceramics

The structures of the *a*-CCTO and CCTO ceramic powders were characterized by X-ray powder diffraction using a Philips X'Pert diffractometer with Cu K_α radiation operated at 40 kV and 40 mA. To study the dielectric properties of the *a*-CCTO and CCTO ceramics, aluminum was evaporated onto both sides of the disks as electrodes. The dielectric properties of the ceramics were determined using an impedance analyzer (Agilent 4294A) at a signal strength of 0.5 Vrms and the frequency ranged from 10^2 Hz to 10^5 Hz at room temperature.

X-ray diffraction characterization of *a*-CCTO and CCTO ceramics

XRD patterns of the *a*-CCTO and CCTO ceramic powders are shown in **Fig. S1**. For the CCTO ceramic, the diffraction pattern could be indexed to a body-centered cubic perovskite-related structure of space group Im3 and the major peaks matched those in the Powder Diffraction File database (PDF 75-2188). No detectable secondary phase was observed. For the *a*-CCTO ceramic, no diffraction peak was detected. The reason for this is that the low sintering temperature of 300 °C cannot generate the ordered crystal lattice.

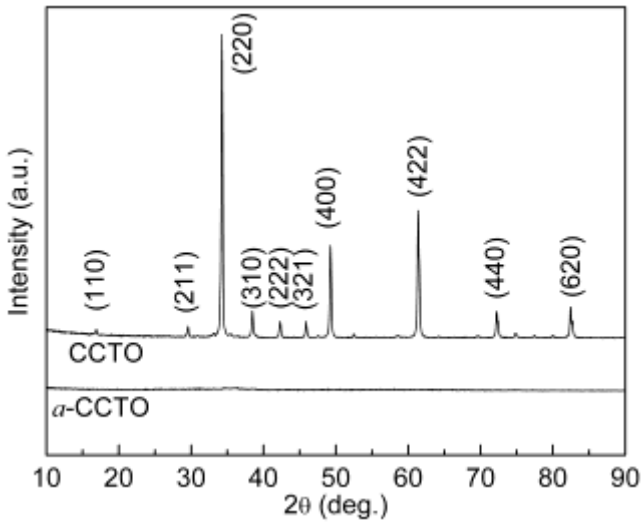

Fig. S1. X-ray powder diffraction patterns of the *a*-CCTO and CCTO ceramics.

Dielectric properties of the *a*-CCTO and CCTO ceramics

The frequency dependence of the dielectric permittivity and the loss in *a*-CCTO and CCTO ceramics are shown in **Fig. S2-S4**. In **Fig. S2**, the CCTO ceramic maintains a high dielectric permittivity of 10^5 and the loss of CCTO in **Fig. S3** decreases when the frequency is less than 1 kHz while it increases when the frequency exceeds 10 kHz. Two dielectric relaxations are thus observed for the CCTO ceramic. The dielectric behavior of CCTO is still controversial.[1-3] Many models accept the internal barrier layer capacitance (IBLC) structure that is composed of semiconducting grains and insulating grain boundaries,[4-6] which can be explained by impedance spectroscopy (IS) and the giant dielectric phenomenon is attributed to the grain boundary layer capacitance. As shown in **Fig. S4**, the grain resistance (R_g) of CCTO is the nonzero intercept on the Z'-axis at the high frequency end (17 Ω). The boundary resistance (R_{gb}) at the low frequency is calculated by extrapolation and is about 2×10^4 Ω. R_{gb} is much larger than R_g, suggesting that CCTO contains semiconducting grains and insulating grain boundaries. Therefore, the IBLC model can explain the dielectric mechanism of the prepared CCTO.

By contrast, the dielectric permittivity of *a*-CCTO decreases rapidly with an increase in frequency as follows: 3×10^4 (1 kHz), 4×10^3 (10 kHz) and 6×10^2 (100 kHz), and this is much lower than that of CCTO. However, at low frequency, the permittivity is even higher than that of CCTO at 100 Hz. High permittivity is generally caused by polarization and different types of polarization present the different frequency dependence and show various dynamic behaviors in the time domain. *a*-CCTO has characteristic structure defects, impurity ions, vacancies and a high defect density because of the larger surface area of the nanosized particles. Dipolar polarization is always associated with the presence of either permanent orientable dipoles or dipolar effects caused by the above-mentioned defects.[7] Therefore, dipolar relaxation may be the dielectric mechanism for *a*-CCTO at low frequency. **Fig. S4** shows that the impedance characteristic of *a*-CCTO is not a semi-circle, indicating that the IBLC model is not suitable for *a*-CCTO. As shown in **Fig. S3**, *a*-CCTO has very high loss. The higher defect density contributes to the higher concentrations of electrons. When an electric field is applied, the leakage current will be enhanced, resulting in higher loss.

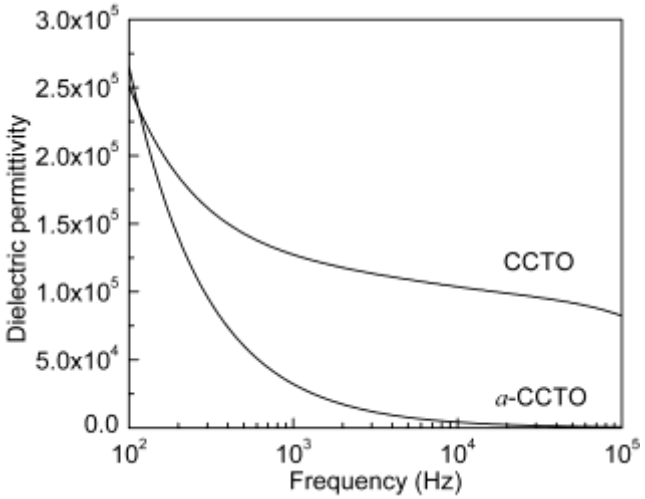

Fig. S2. Dependence of dielectric permittivity on the frequency of *a*-CCTO and CCTO ceramics at room temperature.

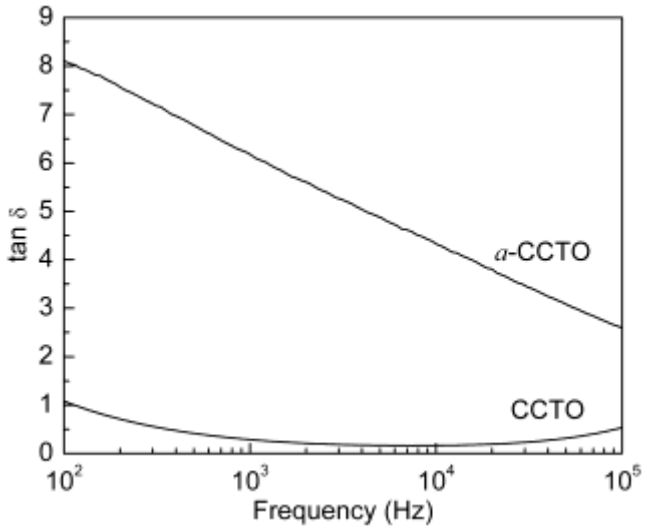

Fig. S3. Dependence of tan δ on the frequency of *a*-CCTO and CCTO ceramics at room temperature.

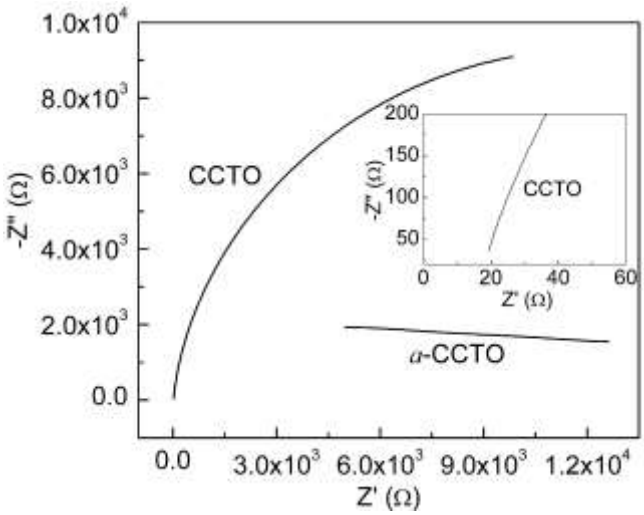

Fig. S4. Impedance complex plane plots for *a*-CCTO and CCTO ceramics at room temperature and the inset shows an expanded view of the high frequency of CCTO data close to the origin.

Dielectric properties of *a*-CCTO/PI and CCTO/PI hybrid films at high concentration

Fig. S5-S7 show the dielectric properties of the *a*-CCTO/PI and CCTO/PI hybrid films at a concentration of 20 vol%. For the *a*-CCTO/PI film, the permittivity is 13 at 100 Hz and this decreases rapidly with increasing frequency. This value is far higher than that of the CCTO/PI film at all frequencies and also higher than that of the CCTO/PI film at a concentration of 20

vol% as prepared by Dang *et al.*[8] However, dielectric loss is high (nearly 0.15 at 100 Hz) and this may be due to the high loss of *a*-CCTO ceramics and the severe agglomeration phenomenon in the film at a concentration of 20 vol%. In **Fig. S7**, the conductivity of the *a*-CCTO/PI film remains low, indicating the good insulation property of the *a*-CCTO/PI film.

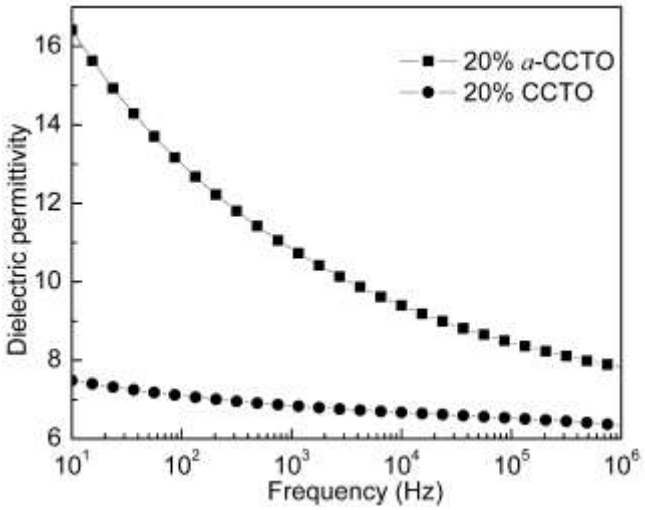

Fig. S5. Dependence of dielectric permittivity on the frequency of the *a*-CCTO/PI and CCTO/PI hybrid films at a concentration of 20 vol% and at room temperature.

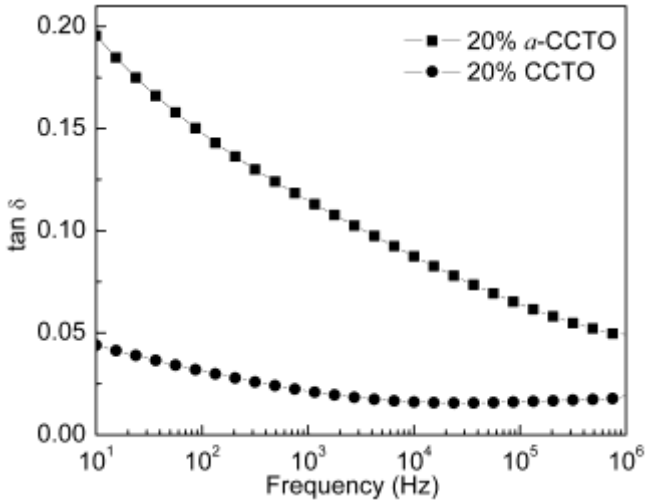

Fig. S6. Dependence of tan δ on the frequency of the *a*-CCTO/PI and CCTO/PI hybrid films at a concentration of 20 vol% and at room temperature.

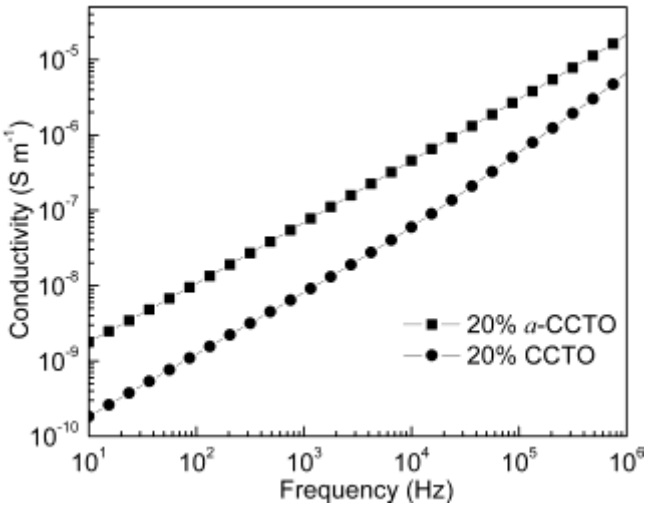

Fig. S7. Dependence of conductivity on the frequency of the *a*-CCTO/PI and CCTO/PI hybrid films at a concentration of 20 vol% and at room temperature.

Notes and references

1 Y. Zhu, J. C. Zheng, L. Wu, A. I. Frenkel, J. Hanson, P. Northrup and W. Ku, *Phys. Rev. Lett.*, 2007, **99**, 037602-1~4.

2 J. L. Zhang, P. Zheng, C. L. Wang, M. L. Zhao, J. C. Li and J. F. Wang, *Appl. Phys. Lett.*, 2005, **87**, 142901~1-3.

3 S. F. Shao, J. L. Zhang, P. Zheng, W. L. Zhong and C. L. Wang, *J. Appl. Phys.*, 2006, **99**, 084106~1-11.

4 B. Shri Prakash and K. B. R. Varma, *J. Mater. Sci*., 2007, **42**, 7467-7477.

5 T. B. Adams, D. C. Sinclair and A. R. West, *Adv. Mater*., 2002,**14**, 1321-1323.

6 M. Li, Z. J. Shen, M. Nygren, A. Feteira, D. C. Sinclair and A. R. West, *J. Appl. Phys*., 2009, **106**, 104106~1-8.

7 L. Fang, M R. Shen, F. A. Zheng, Z. Y. Li and J. Yang, *J. Appl. Phys*., 2008, **104**, 164110~1-8.

8 Z. M. Dang, T. Zhou, S. H. Yao, J. H. Yuan, J. W. Zha, H. T. Song and J. Y. Li, *Adv.*

Mater., 2009, **21**, 2077-2082.